

Supporting information

Experimental procedure

2.1 Chemicals

Absolute ethanol (ACS reagent), $\text{K}_2\text{C}_4\text{TiO}_9 \cdot 2\text{H}_2\text{O}$ ($\geq 98.0\%$), tetraethyl orthosilicate (TEOS, 98%), diethylene glycol (DEG, $\geq 99.5\%$), 2-propanol (anhydrous, 99.5%), WCl_6 ($\geq 99.9\%$), NH_3 (28 wt%), NaOH (pellets EMPLURA®) and HCl (37 wt%) were all purchased from Sigma–Aldrich. All the reagents were used as received. Milli–Q water was collected from a Millipore academic purification system with resistivity 18.2 M Ω cm.

2.2 Method

2.2.1 Synthesis of TiO_2 microspheres. Typically, 0.2 g of $\text{K}_2\text{C}_4\text{TiO}_9$ and 100 mL of H_2O were mixed and stirred until a clear solution was obtained. Then, 150 mL of DEG and 2-propanol, respectively, were added and stirred until a homogeneous yellow solution was obtained. The solution was then transferred into a 100 mL Teflon–lined stainless–steel autoclave and treated at 190 °C for 12 h. After the hydrothermal treatment, yellowish orange powder was obtained and washed three times with ethanol and water, respectively. After drying the powder obtained in an oven at 75 °C, the product was calcined at 500 °C with ramping 10 °C min^{-1} and maintained at 500 °C for 4 h.

2.2.2 Synthesis of $\text{TiO}_2/\text{SiO}_2$ microspheres. The synthesis of $\text{TiO}_2/\text{SiO}_2$ microspheres was prepared according to a previous study.¹ Briefly, an ethanol dispersion of TiO_2 microspheres (3.0 mL, 0.05 g mL^{-1}) was added into a round bottom flask containing ethanol (280 mL), Milli–Q water (70 mL) and NH_3 (5.0 mL, 28 wt%) under ultrasound for 30 min (solution A). After that, 4.0 mL of TEOS was added into the solution A with a flow rate 0.4 mL min^{-1} . Then, the solution was kept under continuous mechanical stirring for 12 h at room temperature. The resultant $\text{TiO}_2/\text{SiO}_2$ microspheres were separated using a centrifuge (ThermoFisher Sorvall Biofuge Primo Benchtop Centrifuge, 4000 rpm for 15 min), followed by washing with three times of Milli–Q water and absolute ethanol, respectively.

2.2.3 Synthesis of $\text{TiO}_2/\text{SiO}_2/\text{W}_{18}\text{O}_{49}$ microspheres. The product of $\text{TiO}_2/\text{SiO}_2$ microspheres obtained was re–dispersed into ethanol (200 mL) and mixed with concentrated NH_3 (0.9 mL, 28 wt%) under ultrasound for 30 min (solution B). After that, 2.0 mL of WCl_6 solution (2.0 g in 100 mL of ethanol) was added in solution B with a flow rate of 0.4 mL min^{-1} . Then, the solution was transferred for solvothermal treatment at 180 °C for 6, 12 or 24 h (denoted as TW x h, in which x is the solvothermal treatment time) to manipulate the thickness of the $\text{W}_{18}\text{O}_{49}$. The resultant $\text{TiO}_2/\text{SiO}_2/\text{W}_{18}\text{O}_{49}$ microspheres were separated using centrifuge, followed by washing with three times of Milli–Q water and absolute ethanol, respectively.

2.2.4 Removal of SiO_2 barrier. The $\text{TiO}_2/\text{W}_{18}\text{O}_{49}$ microspheres were synthesized using an alkaline hydrothermal etching assisted crystallisation method. The $\text{TiO}_2/\text{SiO}_2/\text{W}_{18}\text{O}_{49}$ product obtained in the previous step was mixed with an aqueous NaOH solution (20 mL, 1.0 M), then the solution was transferred to a 100 mL Teflon–lined stainless–steel autoclave. The autoclave was heated at 150 °C for 24 h, and then allowed to cool down to room temperature. Then, the product obtained was immersed in aqueous HCl (100 mL, 0.1 M) for 20 min, and subsequently washed with Milli–Q water until pH value was close to 7, and then dried at 75 °C.

2.3 Characterisation

The morphology of the synthesized products was examined by a field emission scanning electron microscopy (FE–SEM, Quanta 200 F FEI), a high resolution transmission electron microscope (HRTEM, FEI Titan Themis 200) equipped with an energy–dispersive X–ray spectroscopy (EDX) detector operated at 200 kV. To investigate the interior structures of the nanospheres, samples were embedded in TAAB 812 resin and sliced into ~90 nm thick sections. The sliced sections were mounted on the TEM copper grid. Crystallinity and phase identification of the synthesized products were conducted using powder X–ray diffraction XRD (Bruker D8 Advanced Diffractometer) equipped with Cu $\text{K}\alpha$ radiation ($\lambda = 1.5418 \text{ \AA}$) and compared with the ICDD–JCPDS powder diffraction file database. The *in situ* PXRD was carried out at the Australian Synchrotron on the Powder Diffraction beamline. The X–ray energy was 18 keV, and the wavelength ($\lambda = 0.590928 \text{ \AA}$) was calibrated by using a LaB_6 standard (NIST SRM 660b). The methodology was similar to previous *in situ* PXRD studies.^{2–4} The precursor sample ($\text{TiO}_2/\text{SiO}_2$ dispersed in ethanol) was loaded into a quartz glass capillary (1.0 mm OD and 0.02 mm wall thickness). Then, WCl_6 solution was injected into the quartz glass capillary. The loaded capillary was placed at the X–ray beam center and heated (10 °C min^{-1}) to the target temperature (180 °C) by a hot air blower

under the capillary. The temperature was sensed by a K-type thermocouple about 2 mm beneath the capillary and was calibrated by using a KNO_3 temperature standard. *In situ* PXRD patterns were collected during the solvothermal process using a position-sensitive MYTHEN detector over the 2θ range $1.5\text{--}81.5^\circ$ with a time resolution of 2 min. Raman spectroscopy was conducted on a Renishaw InVia Raman Microscope with an excitation source of 785 nm. Diffuse reflectance was collected using a UV-vis spectrometer (Perkin-Elmer Lambda 900) equipped with an integrating sphere (150 mm). X-ray photoelectron spectroscopy (XPS) was performed on a Scienta 300 XPS machine incorporating with a rotating AlK α X-ray source operating at 13 kV \times 333 mA (4.33 kW). Electron analysis is done using a 300 cm radius hemispherical analyser and lens system. The electron counting system consists of a multichannel plate, phosphorescent screen and CCD camera. All multichannel detection counting is done using proprietary Scienta software. The elements present were determined *via* a wide energy range survey scan (200 mV step, 20 ms. dwell time, 150 eV pass energy and summed over 3 scans). The high resolution scans were performed at a similar pass energy (150 eV) but a step size of 20 mV, a dwell time of 533 ms. and summed over 3 scans. The instrument operated at a base pressure of 1×10^{-9} mbar, the energy scale is calibrated using the Au 4_f, Ag 3_d and Cu 2_p emission lines. The half width of the Au 4_f emission line is ~ 1.0 eV. All of the sample was mixed with a small amount of Ag powder to act as a binding energy reference. All data analysis and peak fitting were performed using the CasaXPS software. The photoelectrochemical (PEC) measurement was carried out on the Autolab PGSTAT 302N electrochemical workstation with a standard three-electrode system. To fabricate the working electrode, 1 mg of powder sample was dispersed in 0.5 mL of ethanol followed by sonication for 15 min. The solution obtained was drop-casted onto a piece of fluorine doped tin oxide (FTO) glass to coat an area with dimension 1 cm \times 1 cm. Then, the prepared film was air dried and annealed at 200 $^\circ\text{C}$ for 1 h. Pt wire and Ag/AgCl (KCl 1 M) were used as the counter and reference electrodes, respectively. The electrolyte used was 0.5 M of Na_2SO_4 aqueous solution. The PEC measurement was conducted in the presence of solar simulator (Newport 92250A; AM 1.5G; 100 mW cm^{-2}). *Operando* Diffuse Reflectance Infrared Fourier Transform Spectroscopy (DRIFTS) experiments were conducted on Agilent Cary 600 series spectrometer equipped with Harrick Praying Mantis reaction cell. The gas inlet of the cell was directly connected to a flow system equipped with mass flow controllers and a temperature controller. The cell outlet was connected to the mass spectrometer Hiden QGA MS. In each experiment, 20 mg of catalyst powder was placed in the cell. Before reaction, the KBr background was collected in presence of CO_2 which was flowing through bubbler. 64 scans were collected per spectrum with a spectral resolution of 4 cm^{-1} and in the spectral range of 4000–400 cm^{-1} .

2.4 Photocatalytic testing

CO_2 photoreduction testing of the fabricated samples was conducted in a customised stainless steel photoreactor with a quartz window.⁵ 0.01 g of sample was distributed as powder on the bottom of the photoreactor. To purge and equilibrate the system, a flow rate of 0.42 mL min^{-1} CO_2 was passed through an aluminium bubbler set at 20 ± 2 $^\circ\text{C}$ and the charged photoreactor overnight. The reaction was performed at 80 ± 2 $^\circ\text{C}$, which was controlled by a hot plate placed under the photoreactor. An optical fibre lamp (OmniCure S2000) was used as the light source (135 mW cm^{-1} , 400–500 nm). The irradiance was measured using a radiometer (OmniCure R2000). The outlet gas was analysed hourly online by a gas chromatography (GC, Agilent, Model 7890 B series) with a Hayesep Q column (1.5 m, 1/16 inch OD, 1 mm ID), Molecular Sieve 13X (1.2 m, 1/16 inch OD, 1 mm ID), thermal conductivity detector (TCD), nickel catalysed methaniser and flame-ionization detector (FID).

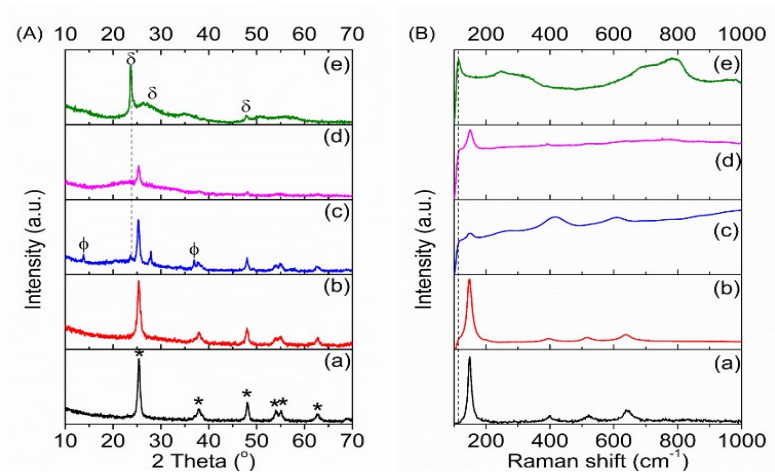


Figure S1. Laboratory-based PXRD (A) and Raman (B) patterns of TiO₂ (a), TW6h (b), TW12h (c), TW24h (d) and pristine W₁₈O₄₉ (e). *Represents the anatase phase of TiO_{2-x}, φ represents WO₃ and δ represents W₁₈O₄₉. The black dashed lines are for guidance.

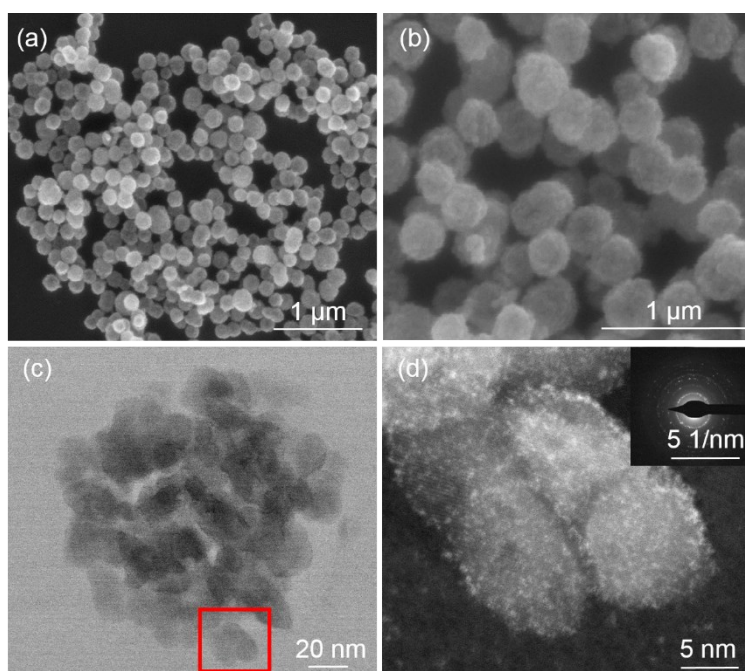


Figure S2. SEM (a and b) and TEM images of TiO₂ (c) and the selected area in the red box (d) with the corresponding SAED (inset in d).

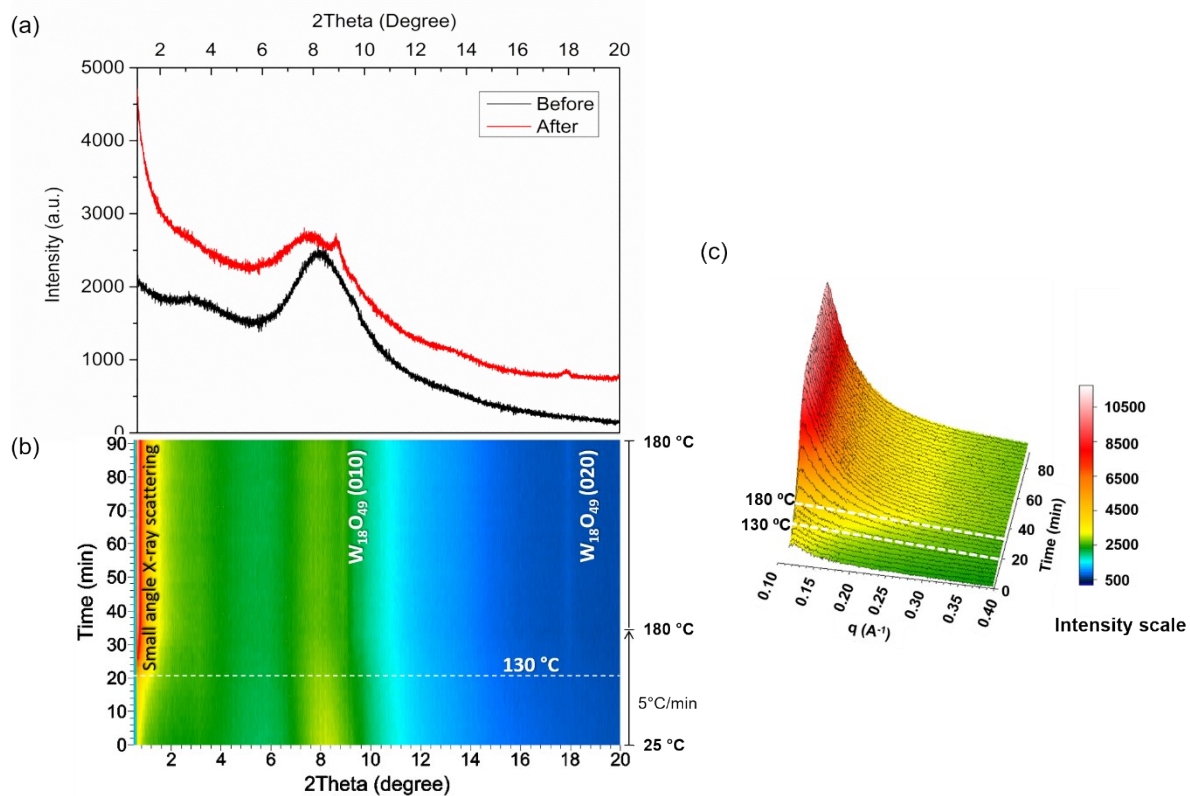


Figure S3. Synchrotron *in situ* PXRD pattern (a, b) and the small angle region (c) of TiO_2 - SiO_2 loaded in the WCl_6 -ethanol solution.

The *in situ* experiment was performed using as-prepared yellow TiO_{2-x} coated with SiO_2 . The peaks centred at $\sim 3.4^\circ$ and $\sim 9.9^\circ$, which were assigned to the (001) and (110) planes, were observed (Figure S3a, JCPDS: 11-0217). The crystallisation of $W_{18}O_{49}$ was observed when the temperature approached 130°C , in which the peaks centred at $\sim 9.2^\circ$ and 18° corresponded to the (010) and (020) planes of $W_{18}O_{49}$, respectively. Similarly, the emergence of peak in the small angle region ($<1^\circ$) was also observed when the temperature achieved 130°C .

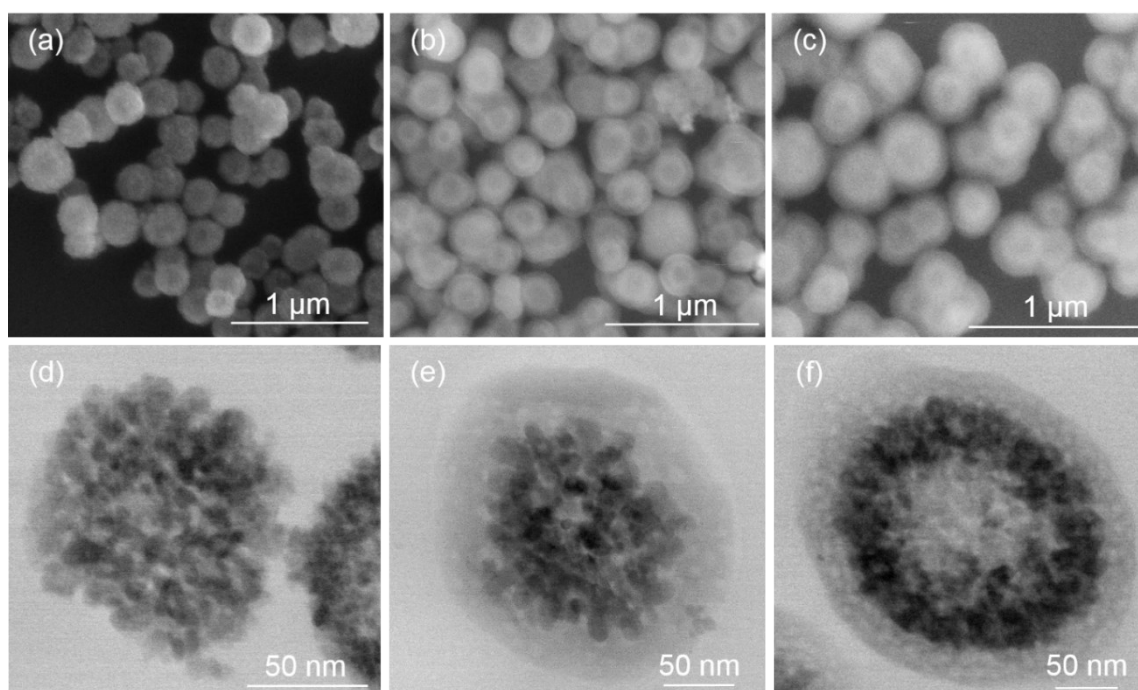


Figure S4. SEM and TEM images of TW6h (a, d), TW12h (b, e) and TW24h (c, f) after the removal of SiO_2 .

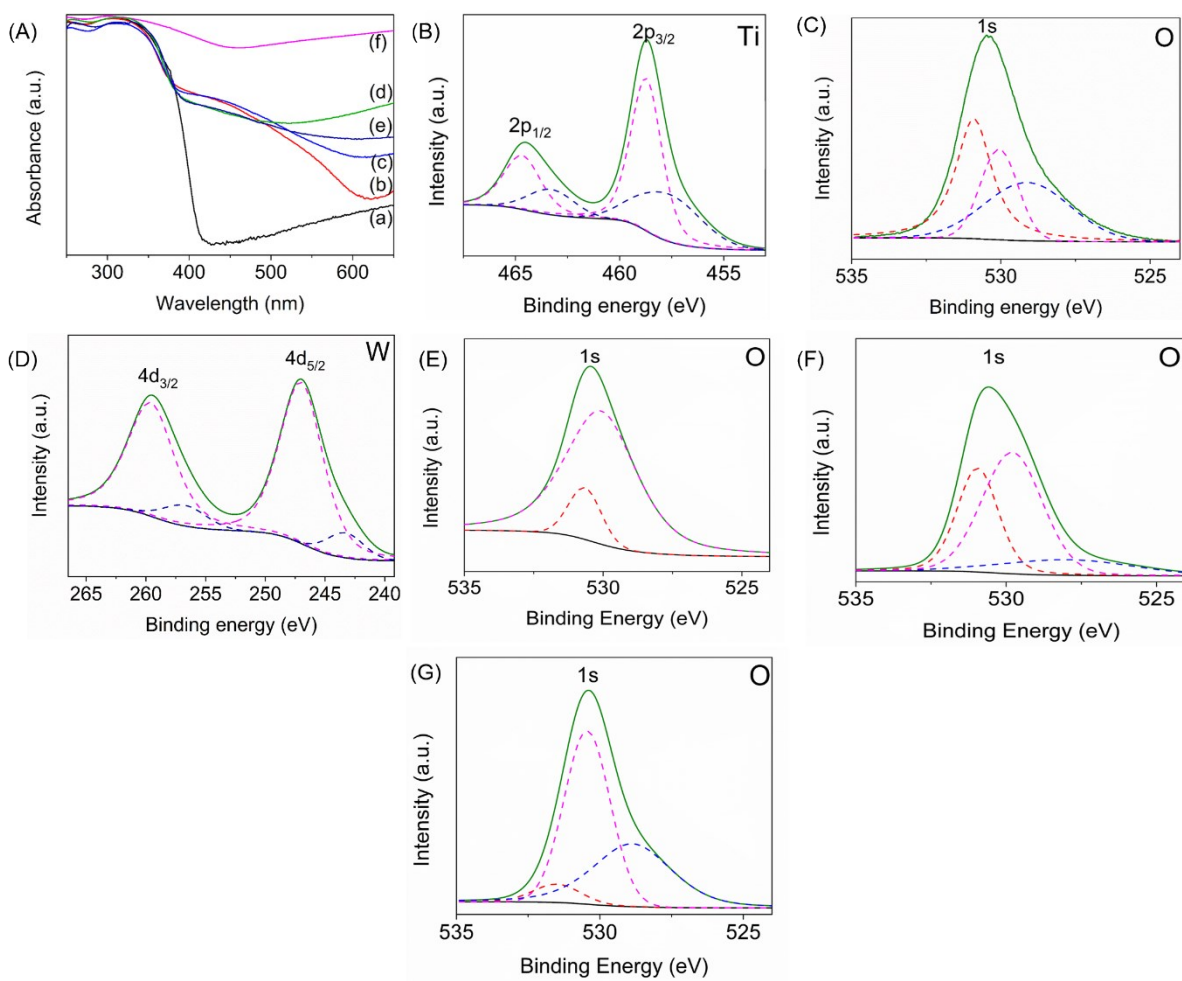


Figure S5. Absorbance spectra (A) of P25 (a), pristine TiO_{2-x} (b), TW6h (c), TW12h (d), TW24 (e) and $\text{W}_{18}\text{O}_{49}$ (f). High resolution XPS Ti (B), O (C) and W (D) spectra of TW12h. High resolution XPS O spectra of pristine TiO_{2-x} (E), TW6h (F), and TW24h (G).

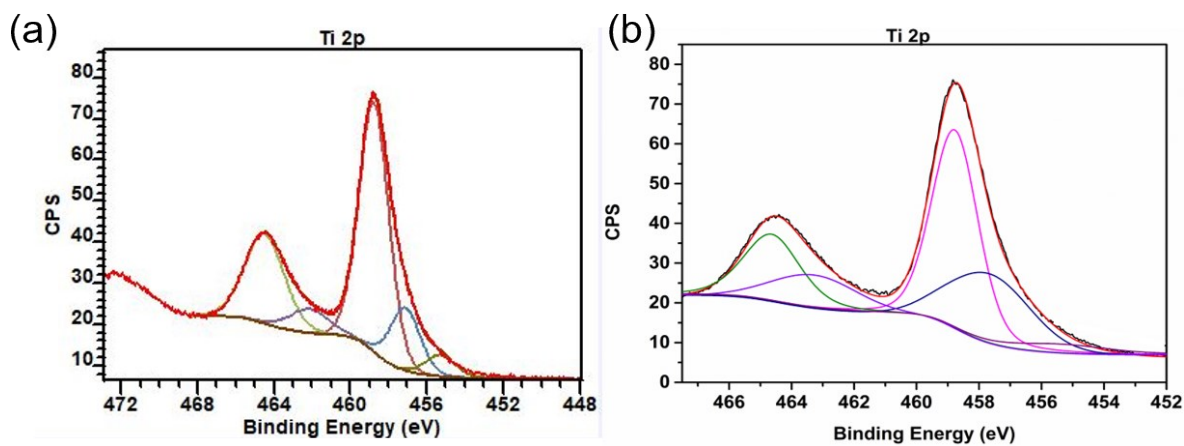


Figure S6. High resolution XPS Ti spectrum of the as-prepared TiO_2 (a) and TW6h (b).

The high resolution Ti spectrum was deconvoluted into 5 peaks, which were centred at 455.3, 457.4, 458.8, 461.8 and 464.2 eV. The peaks centred at 458.8 and 464.2 eV corresponded to the typical Ti^{4+} moiety in TiO_2 .⁶ Meanwhile, the peaks observed at the lower binding energy were attributed to the oxidised species of Ti^{3+} (457.4 and 461.8 eV) and Ti^{2+} (455.3 eV) moieties.⁶⁻⁹

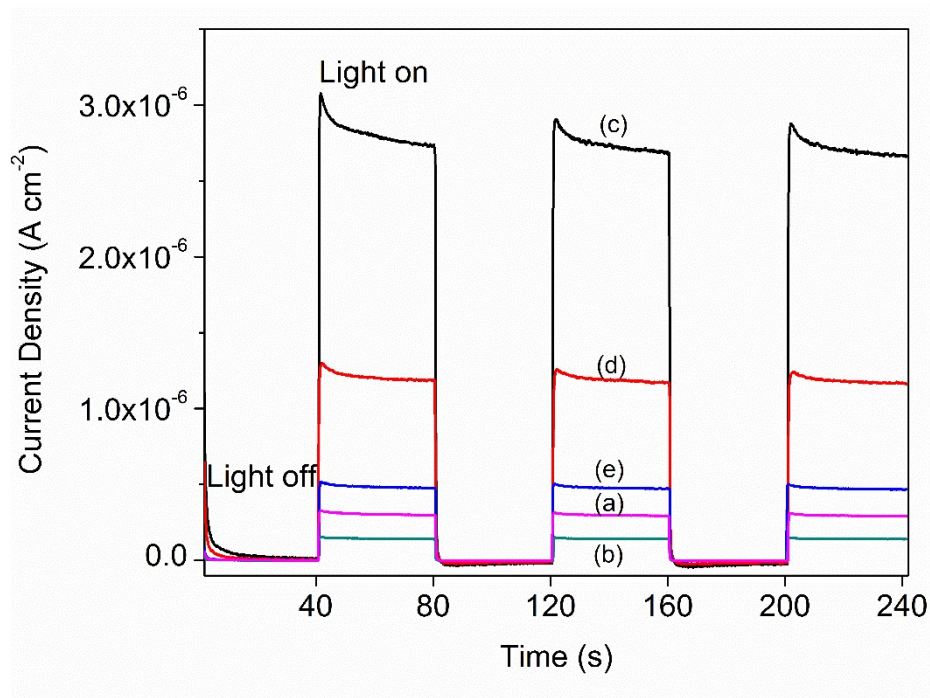


Figure S7. PEC pattern of the as-prepared TiO_2 (a), pristine $\text{W}_{18}\text{O}_{49}$ (b), TW6h (c), TW12h (d) and TW24h (e).

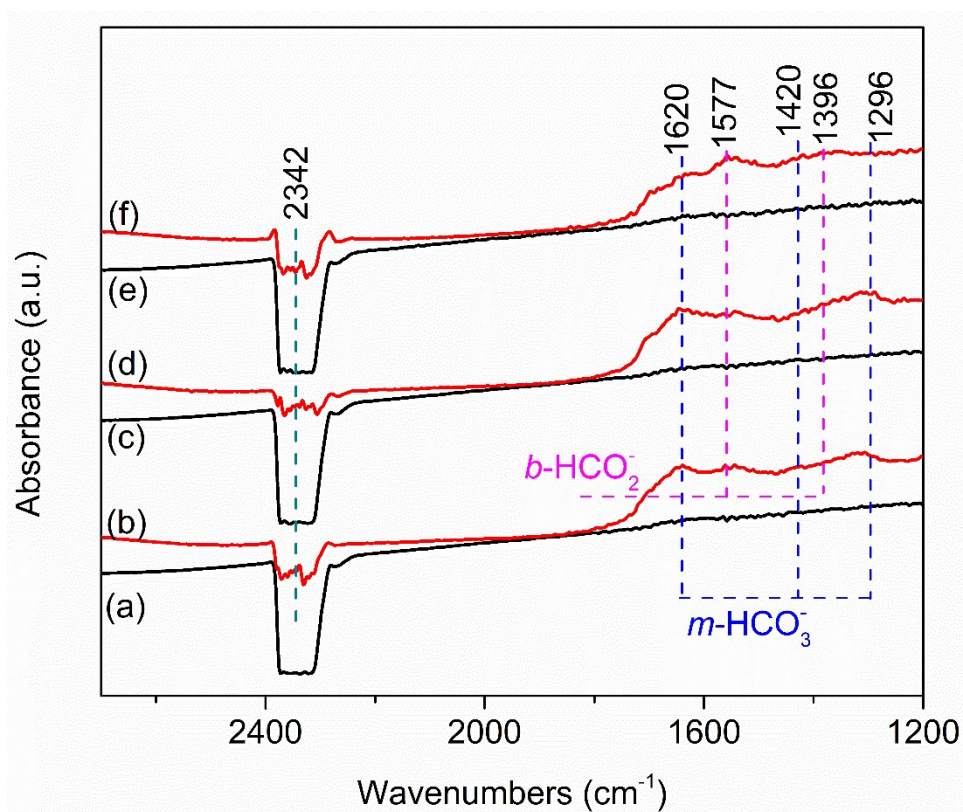
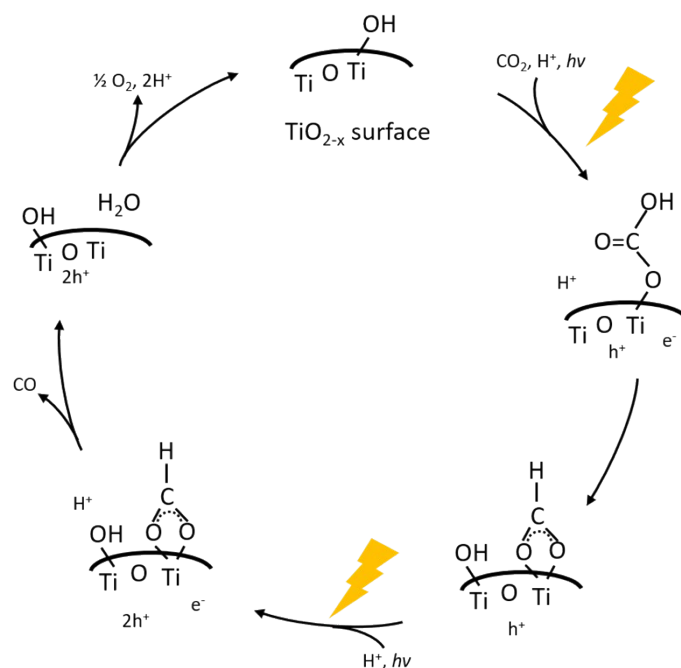
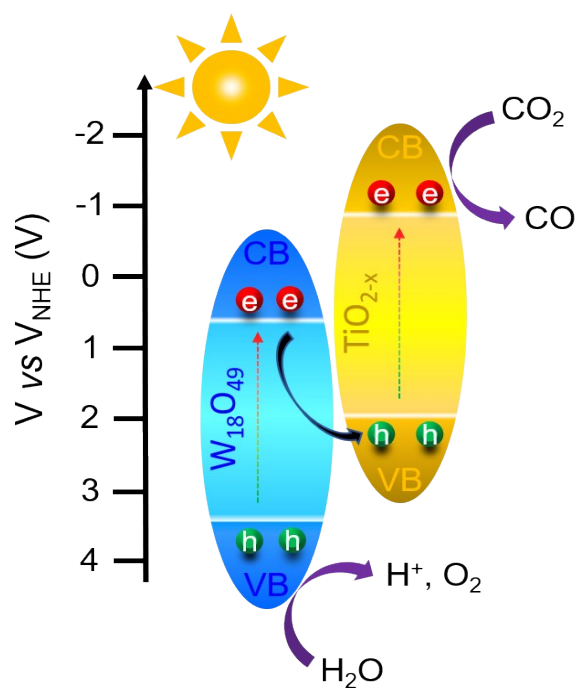


Figure S8. Operando DRIFT spectra of P25 (black) and TiO_{2-x} (red) at 24 °C when light is off (a, b) and on (c, d); and at 80 °C (e, f) when light is on.



Scheme S1. Proposed CO₂ photoreduction reaction on the pristine TiO_{2-x}.



Scheme S2. Proposed CO₂ photoreduction reaction of the fabricated TW_xh samples.

Reference:

1. W. Li, Y. Deng, Z. Wu, X. Qian, J. Yang, Y. Wang, D. Gu, F. Zhang, B. Tu and D. Zhao, *J. Am. Chem. Soc.*, 2011, **133**, 15830-15833.

2. J. Z. Y. Tan, N. M. Nursam, F. Xia, M.-A. Sani, W. Li, X. Wang and R. A. Caruso, *ACS Appl. Mater. Interfaces*, 2017, **9**, 4540-4547.
3. J. Z. Y. Tan, N. M. Nursam, F. Xia, Y. B. Truong, I. L. Kyratzis, X. Wang and R. A. Caruso, *J. Mater. Chem. A*, 2017, **5**, 641-648.
4. F. Xia, D. Chen, N. V. Y. Scarlett, I. C. Madsen, D. Lau, M. Leoni, J. Ilavsky, H. E. A. Brand and R. A. Caruso, *Chem. Mater.*, 2014, **26**, 4563-4571.
5. W. A. Thompson, C. Perier and M. M. Maroto-Valer, *Appl. Catal., B*, 2018, **238**, 136-146.
6. P. Finetti, F. Sedona, G. A. Rizzi, U. Mick, F. Sutara, M. Svec, V. Matolin, K. Schierbaum and G. Granozzi, *J. Phys. Chem. C*, 2007, **111**, 869-876.
7. Y. Hasegawa and A. Ayame, *Catal. Today*, 2001, **71**, 177-187.
8. Z. Luan, E. M. Maes, P. A. W. van der Heide, D. Zhao, R. S. Czernuszewicz and L. Kevan, *Chem. Mater.*, 1999, **11**, 3680-3686.
9. J. Matharu, G. Cabailh and G. Thornton, *Surf. Sci.*, 2013, **616**, 198-205.